Parsimonious Refraction Interferometry

Sherif M. Hanafy and Gerard Schuster. King Abdullah University of Science and Technology (KAUST).*

Summary

We present parsimonious refraction interferometry where a densely populated refraction data set can be obtained from just two shot gathers. The assumptions are that the first arrivals are comprised of head waves and direct waves, and a pair of reciprocal shot gathers is recorded over the line of interest. The refraction traveltimes from these reciprocal shot gathers can be picked and decomposed into $O(N^2)$ refraction traveltimes generated by N virtual sources, where N is the number of geophones in the 2D survey. This enormous increase in the number of virtual traveltime picks and associated rays, compared to the $2N$ traveltimes from the two reciprocal shot gathers, allows for increased model resolution and better condition numbers in the normal equations. Also, a reciprocal survey is far less time consuming than a standard refraction survey with a dense distribution of sources.

Introduction

Refraction tomography is one of the most widely used imaging tools in earthquake studies (Stein and Wysession, 2003), crustal-mantle imaging (Prodehl and Mooney, 2012), exploration geophysics (Yilmaz, 2001), and engineering seismology (Yilmaz, 2015). For 2D engineering seismology, receivers are deployed along a line and common shot gathers (CSGs) are recorded for source positions at selected positions on the line. To save costs, a parsimonious survey is carried out where sources are located only at each end of the receiver line as shown in Figure 1. The first breaks are picked from each shot gather and the traveltimes are inverted by a simple formula that assumes a layered model with an unknown dip angle for each interface. These two shot gathers are denoted as a pair of reciprocal shot gathers. Parsimonious surveys save time, but at the cost of less slowness resolution and certainty in the estimate of the subsurface model.

We now propose the creation of virtual shot gathers which give almost as much refraction information as a full survey with N shots, where a shot is located at each of the N geophone locations. The result is a tomogram with denser ray coverage and better resolution in the tomogram compared to that from the original data. We call this procedure parsimonious interferometry because it uses a stationary phase principle to decompose the reciprocal traveltime data into virtual traveltimes associated with shorter raypaths. Unlike the original pair of reciprocal shots, the virtual shot locations are at all of the geophone locations.

The next section describes the theory of parsimonious refraction interferometry. It is a special case of Fermat's interferometric traveltime principle (Schuster, 2005) and closure phase (Schuster et al., 2014) that allows for the decomposition of long raypaths and traveltimes into, respectively, shorter raypaths and traveltimes. Instead of body wave traveltimes we now apply it to traveltimes of head waves. Section 3 presents the results of applying parsimonious interferometry to both synthetic data and field data. The final section presents a summary and conclusions.

Theory

Assume two reciprocal sources and the checkerboard layered medium in Figure 1, where head waves propagate along the interface between the upper and lower layers. There can be lateral velocity variations in the upper medium and there are N evenly spaced geophones on the recording surface between the two sources. The head-wave traveltime from the source at A to the geophone at C is given by

$$\tau_{AC} = \tau_{Ax'} + \tau_{x'x} + \tau_{xC}, \qquad (1)$$

and the reciprocal traveltime from D to B is

$$\tau_{DB} = \tau_{Dx} + \tau_{x'x} + \tau_{x'B}, \qquad (2)$$

where $\tau_{x'x}$ is the traveltime from x to x' along the refraction ray. Reciprocity demands that $\tau_{x'x} = \tau_{xx'}$.

To create virtual sources and receivers within the array, we define the stationary interferometric condition for the postcritical geophone locations C and B between the reciprocal sources at A and D:

$$|C - A| + |B - D| > |A - D|, \qquad (3)$$

which means that C is to the right of B. We also demand that C and B are separated by a critical offset where a refraction arrival would be recorded at B if a source was placed at C. Subtracting the reciprocal traveltime $\tau_{AD} = \tau_{Ax'} + \tau_{x'x} + \tau_{xD}$ from the sum $\tau_{AC} + \tau_{DB}$ gives the stationary interferometric traveltime $\delta\tau_{CB}$ (see Figure 10 in Schuster et al. (2014)):

$$\begin{aligned}\delta\tau_{CB} &= \tau_{AC} + \tau_{DB} - \tau_{AD},\\ &= \tau_{Ax'} + \tau_{x'x} + \tau_{xC} + [\tau_{Dx} + \tau_{xx'} + \tau_{x'B}] - \tau_{Ax'} - \tau_{x'x} - \tau_{xD},\\ &= \tau_{Cx} + \tau_{xx'} + \tau_{x'B}, \qquad (4)\end{aligned}$$

where B is at a postcritical distance to the left of C. $\delta\tau_{CB}$ is denoted as an interferometric stationary traveltime because

the reciprocal raypath $\overline{Ax'xD}$, marked by the dashed red ray in Figure 1, cancels the phase associated with the common raypaths of the purple $\overline{Ax'xC}$ and green $\overline{Dxx'B}$ rays. The result is the virtual traveltime $\delta\tau_{CB}$ associated with the much shorter raypath $Cxx'B$ denoted by the dashed blue ray. Thus, $\delta\tau_{CB}$ is associated with a virtual source at C exciting a virtual refraction arrival that is recorded at B. This natural redatuming operation is the key principle underlying seismic interferometry (Snieder, 2004; Wapenaar, 2004).

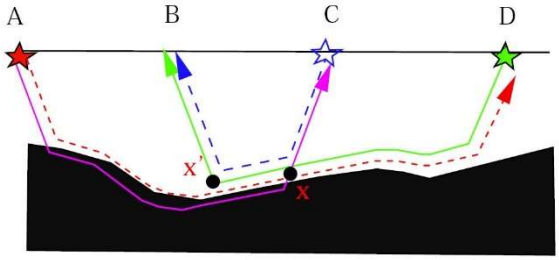

Figure 1: Two-layer model where the black medium is faster than the top layer; the reciprocal sources are at A and D and are associated with the dashed red ray. The dashed blue raypath is associated with the virtual refraction ray that is excited by the virtual source (blue star) at C and terminates at B. Illustration adapted from Figure 10 in Schuster et al. (2014).

Equation 4 satisfies Fermat's interferometric principle (Schuster, 2005) because the subtraction of τ_{AD} (red dashed ray) from $\tau_{AC} + \tau_{AB}$ (solid green and purple rays) gives the same value of $\delta\tau_{CB}$ for all postcritical, i.e. stationary, locations of the reciprocal sources.

Therefore, equation 4 can be used to generate $O(N)$ virtual shot gathers, where the number of reciprocal geophone pairs that satisfy the stationary interferometic condition in equation 3 is assumed to be nearly equal to the number N of geophones in the survey. Each virtual shot gather will, on average, contain $O(N/2)$ virtual traveltimes generated by equation 4. This means that parsimonious interferometry can create $O(N^2)/2$ virtual refraction traveltimes from the $2N$ traveltimes picked from two reciprocal shot gathers. This abundance of new traveltimes can be used to invert for the subsurface velocity model with much greater ray density and better model resolution than inverted from the original data set. The above analysis assumed only one refractor, but it can be extended to models with multiple refractors.

Figure 2a shows that a reciprocal pair of shot gathers can give rise to gaps in the illumination zones of the direct arrivals and refractions. For refractions, these gaps can be caused by the inability to pick far-offset traveltimes as indicated by the truncated green lines in Figure 2a. This problem can be partly remedied if the later-arriving direct waves and refractions can be picked, as illustrated by the dashed lines in Figure 2b.

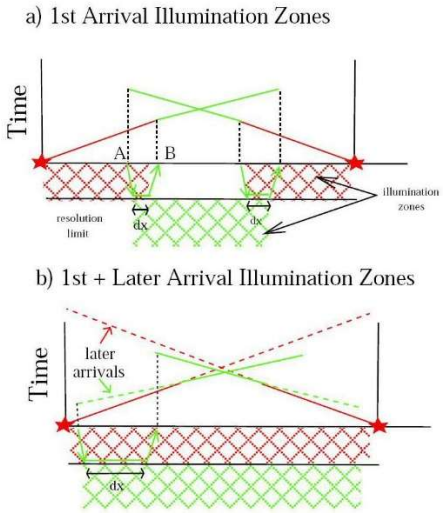

Figure 2: Hatched illumination zones for traveltimes picked from a) first arrivals and b) both first and the dashed later arrivals. The red (green) lines indicate direct-wave (refraction) arrivals. The horizontal resolution limit dx is denoted by black two-sided arrows for different portions of the subsurface. The resolution limit dx cannot be less than the distance between adjacent geophones.

Numerical Results

Parsimonious interferometry will be tested on two models, one is a simple two-layered velocity model and the other is a complicated velocity model. In each case the traveltimes were generated using a finite-difference solution to the eikonal equation. The final example is for refraction data collected near the Gulf of Aqaba.

1. First Synthetic Example: Two-Layer Model

The two-layer model is shown in Figure 3a and a finite-difference solution (Qin et al., 1991) to the eikonal equation is used to compute 120 shot gathers of first-arrival traveltimes, with a source located every 5 m. The geophones are placed every 5 meters on the surface. The 240 first-arrival traveltimes from the two reciprocal shot gathers, where one source is at (0, 0) and the other is at (0, 600 m), were then inverted by traveltime tomography to get the reciprocal tomogram in Figure 3b. In this case there is a poor correspondence between the reciprocal tomogram and the actual velocity model. For comparison, Figure 3c shows the standard tomogram inverted from 14,400 actual traveltimes generated by placing shots at each of the 120 geophones. As expected, the standard tomogram mostly agrees with the actual velocity model.

Equation 4 is then used to compute the virtual traveltimes from the 240 traveltimes associated with the two reciprocal

shot gathers. The result is the creation of *O*(14,000) virtual traveltimes computed for virtual shots at each of the geophones. These virtual traveltimes agree with the actual ones to within a maximum error of less than 0.1 ms, and the virtual tomogram is shown in Figure 3d. As expected, there is a close correspondence between the standard and virtual tomograms.

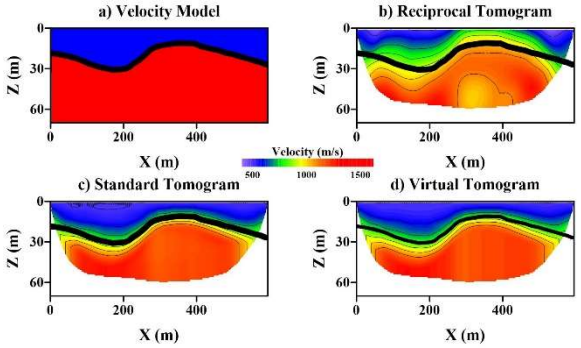

Figure 3: a) Two-layer model, b) reciprocal tomogram inverted from the 240 traveltimes in the two reciprocal shot gathers, c) standard tomogram inverted from the 14,400 actual traveltimes in 120 shot gathers, with a shot at each geophone location. d) Virtual tomogram inverted from O(14,000) virtual traveltimes created from 240 reciprocal traveltimes.

2. Second Synthetic Example: Aqaba Model

Parsimonious interferometry is also tested on the Aqaba velocity model in Figure 4a, which is based on a tomogram inverted from a refraction survey conducted near the Gulf of Aqaba. The reciprocal traveltimes were picked from two reciprocal shot gathers, which are then inverted to give the Figure 4b tomogram. As expected there is a poor correspondence between this tomogram (Figure 4b) and the velocity model (Figure 4a). In this case there were 120 traveltimes in each reciprocal shot gather for a total of 240 traveltimes.

The traveltimes were then computed for a physical shot at each geophone location to give a total of 120^2 = 14,400 traveltimes. These data were inverted to give the standard P-velocity tomogram in Figure 4c. As expected, there is a much better correspondence with the actual velocity model than seen in the reciprocal tomogram. The virtual traveltimes were then computed from the 240 reciprocal traveltimes to give a total of *O*(14,000) virtual traveltimes. These virtual traveltimes agreed with the actual traveltimes with an average error of 2 ms. The virtual traveltimes for the direct arrivals were computed using the near-surface velocity estimated from the reciprocal traveltimes. All of the virtual traveltimes were then inverted to give the Figure 4d virtual tomogram. There is almost an exact agreement between the standard and virtual tomograms, which is somewhat surprising because some refraction arrivals are associated with diving waves, and the traveltimes of the virtual waves were estimated from the reciprocal traveltimes.

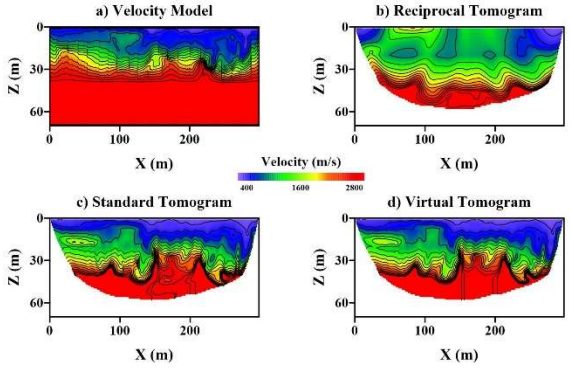

Figure 4: a) Aqaba velocity model, b) reciprocal tomogram inverted from the 240 traveltimes in the two reciprocal shot gathers, c) standard tomogram inverted from the 14, 400 actual traveltimes in 240 shot gathers, with a shot at each geophone location. d) Virtual tomogram inverted from *O*(14,000) virtual traveltimes.

Aqaba Field Survey and Data

A seismic survey was carried out near the Gulf of Aqaba, where 120 geophones are deployed at 2.5 m intervals along a line. A 90 kg accelerated weight drop was used for a source at every geophone position to collect 120 common shot gathers. A total of 14,400 first-arrival traveltimes were picked from the CSGs. The signal-to-noise ratio was excellent so traveltimes could be picked from every trace.

A source at each end of the line was used to form two reciprocal shot gathers. The first-arrival traveltimes were picked and used to compute 14,400 virtual traveltimes from equation 4. Some of these traveltimes are not physically related to refraction times because the receiver-receiver offset is not at a post-critical offset. Such non-physical traveltimes are identified by creating Common Pair Gathers (CPG). A CPG is created by subtracting the virtual traveltimes between a virtual shot and a virtual receiver at B from the traveltime between the same virtual shot and another virtual receiver at C, then repeat this for all possible virtual shot locations. The traveltimes that are equal to one another in the CPG indicate that the associated virtual traveltimes are those from head waves. If a traveltime deviates from the trend then it is rejected.

Due to the long distance between the two shots at the end points of the survey, there will be a gap in the arrival times of the direct waves. To fill in this gap, we used the direct wave traveltimes from 5 CSGs with a shot interval of 60 m. These direct wave traveltimes are then interpolated to other

source locations to fill in the missing direct wave traveltimes in the other virtual CSGs.

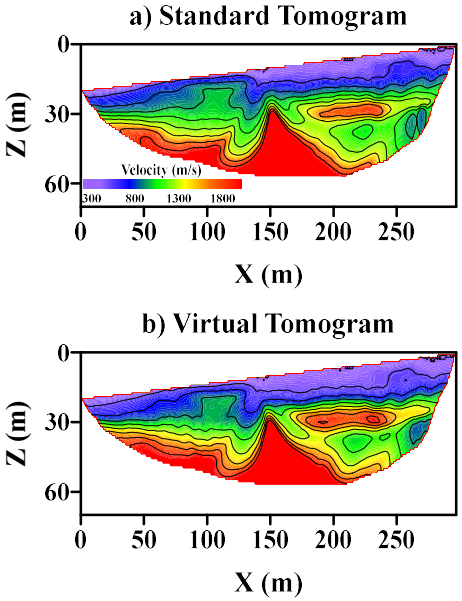

Figure 7: Aqaba tomograms inverted from the a) standard and b) virtual data sets.

Inverting the 14,400 actual and virtual traveltimes by a multiscale tomography method (Nemeth et al., 1997) gives the tomograms shown in Figures 7a and 7b, respectively. It is clear that there is a mostly excellent agreement between the two tomograms. In the standard tomogram, the shooting effort required 1.5 days to conduct, and more than a day of effort was needed for traveltime picking. For the virtual tomogram, we estimate that no more than 1 hour of shooting time and less than 30 minutes of picking time would be needed to record and analyze the reciprocal data set.

Conclusions

The theory of parsimonious interferometry is presented where a dense set of virtual refraction traveltimes is computed from refraction traveltimes picked from a pair of reciprocal shot gathers. In theory, a virtual shot gather of traveltimes can be computed for a virtual shot at each of the geophones in the 2D reciprocal survey. This means that *O(N)* shot gathers of virtual traveltimes can be created from shots placed at each of the N geophones. A key advantage of virtual data is that it acts as a preconditioner to $L^T L$, which reduces the condition number by a factor of three compared to that of the reciprocal data.

Tests with synthetic and field data validate that inversion of virtual refraction traveltimes can give tomograms that closely resemble those computed from traveltimes recorded in a dense survey. If the first arrivals are mostly head-wave arrivals, not strong diving waves, then dense 2D refraction surveys might be replaced by inexpensive reciprocal surveys with as few as two shots placed at each end of the line.

The limitations of parsimonious interferometry are the following.

1. The virtual traveltimes can have three times the variance of the recorded traveltimes for random uncorrelated picking errors.
2. The first arrivals are assumed to be mostly head waves, which is strictly not true for velocities that strongly increase with depth. Surprisingly, our tests suggest that parsimonious tomography has some tolerance to traveltimes associated with diving waves. We don't always expect this type of tolerance for wide-offset refractions from the deep part of a basin or crust.
3. First-arrivals with low signal-to-noise ratios (SNRs) will contain large picking errors at far-offset traces. These large picking errors are expected to propagate to all source-receiver offsets in the virtual data.
4. If the reciprocal pair of shots is too far apart then this will lead to poor lateral resolution and gaps in the illumination of the subsurface. This problem can be partly mitigated by picking later direct and refraction arrivals, or by conducting additional reciprocal surveys with shorter offsets across the survey area.
5. Out-of-the-plane refractions in the reciprocal survey will degrade the accuracy of the virtual refractions.

EDITED REFERENCES

Note: This reference list is a copyedited version of the reference list submitted by the author. Reference lists for the 2016 SEG Technical Program Expanded Abstracts have been copyedited so that references provided with the online metadata for each paper will achieve a high degree of linking to cited sources that appear on the Web.

REFERENCES

Menke, W., 1984, Geophysical data analysis: Discrete inverse theory: Academic Press Inc.

Nemeth, T., E. Normark, and F. Qin, 1997, Dynamic smoothing in crosswell traveltime tomography: Geophysics, **62**, 168–176, http://dx.doi.org/10.1190/1.1444115.

Prodehl, C., and W. D. Mooney, 2012, Exploring the earth's crust: History and results of controlled-source seismology: Geological Society of America, Memoir 208, 764.

Schuster, G. T., 1988, An analytic generalized inverse for common depth point and vertical seismic profile traveltime equations: Geophysics, **53**, 314–325, http://dx.doi.org/10.1190/1.1442465.

Schuster, G. T., 2005, Fermat's interferometric principle for target-oriented traveltime tomography: Geophysics, **70**, no. 4, U47–U50, http://dx.doi.org/10.1190/1.1997368.

Schuster, G., Y. Huang, S. M. Hanafy, M. Zhou, J. Yu, O. Alhagan, and W. Dai, 2014, Review on improved seismic imaging with closure phase: Geophysics, **79**, no. 5, W11–W25, http://dx.doi.org/10.1190/geo2013-0317.1.

Snieder, R., 2004, Extracting the Green's function from the correlation of coda waves: A derivation based on stationary phase: Physical Review E, **69**, 046610, http://dx.doi.org/10.1103/PhysRevE.69.046610.

Stein, S., and M. Wyession, 2003, An introduction to seismology, earthquakes, and earth structure: Blackwell Publishing Company.

Wapenaar, K., 2004, Retrieving the elastodynamic Greens function of an arbitrary inhomogeneous medium by cross correlations: Physical Review Letters, **93**, 254301, http://dx.doi.org/10.1103/PhysRevLett.93.254301.

Yilmaz, O., 2001, Seismic data analysis: SEG Publishing, http://dx.doi.org/10.1190/1.9781560801580.

Yilmaz, O., 2015, Engineering seismology with applications to geotechnical engineering: SEG Publishing, http://dx.doi.org/10.1190/1.9781560803300